Supporting Information

Planar refractive index patterning through microcontact photothermal annealing of a printable organic/inorganic hybrid material

Stefan Bachevillier, Hua-Kang Yuan, Kornelius Tetzner, Donal D. C. Bradley, Thomas D. Anthopoulos, Paul N. Stavrinou, Natalie Stingelin**

Materials: Titanium(IV) tetrachloride (ReagentPlus®; purity > 99.9 %), poly(vinyl alcohol) (PVAl) (Mowiol® 18-88; $M_w \approx 130$ kg·mol^{-1}; residual content of acetyl groups = 10.0 - 11.6 %) were purchased from Sigma-Aldrich.

Hybrid synthesis/film preparation: A hybrid made of poly(vinyl alcohol) (PVAl) cross-linked with 60 vol% titanium oxide hydrate was selected because it was previously established that this composition provides an excellent compromise with respect to film formation, refractive index and optical quality.[1,2] Accordingly, for 10 mL of hybrid solution, 3.4 mL of 2 M titanium oxide hydrate solution, from cold hydrolysis of $TiCl_4$ was slowly added to 6.6 mL of 40 g.L^{-1} PVAl solution under stirring leading to a molecular hybrid of an inorganic content of 25.8 mmol titanium oxide hydrates per 1g PVAl, which corresponds to a hybrid of 60 vol% titanium oxide hydrates. [Note, the most straight-forward manner to express the hybrid concentration is the number of titanium atoms per gram of polymer, expressed as mol Ti/g PVAl. To calculate the volume fraction of the inorganic species, which assists establishing certain structure/property relations, Equation S1 can be used:

$$\%vol\,Ti = \frac{V_{Ti\,species}}{V_{Ti\,species} + V_{PVAl}} \times 100 = \frac{{(n_{Ti\,species}.M_{Ti\,species})}/{\rho_{Ti\,species}}}{{(n_{Ti\,species}.M_{Ti\,species})}/{\rho_{Ti\,species}} + V_{PVAl}} \times 100 \tag{S1}$$

with $M_{Ti\,species} = 90$g.mol^{-1} and $\rho_{Ti\,species}$=1.95kg.m^{-3}. More details can be found in Ref 1.]

A schematic illustration of the resulting hybrid structure is shown in **Fig. S1**. Solutions were spin-coated on glass or silicon/silicon oxide substrates with speeds between 800 and 5000 rpm and dry in air at room temperature. A following ageing in dry vacuum for 7 days at room temperature using a desiccator. Solutions can be stored in the fridge over periods of months, if not years.

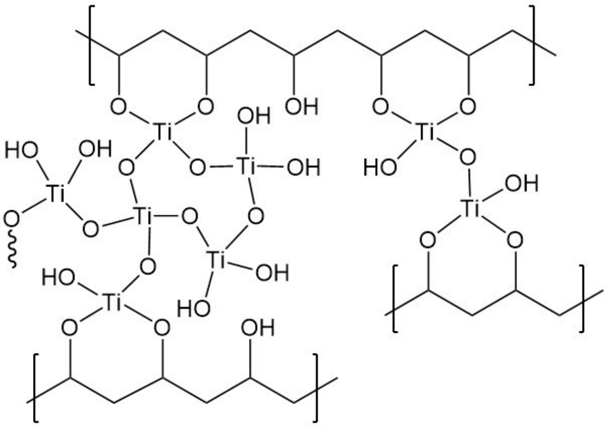

Fig. S1. Chemical structure of the hybrid that is forming between titanium oxide hydrates and poly(vinyl alcohol).[1f,2]

Surface profilometry: Generally, films of a thickness of ≈630 nm to ≈670 nm were used, though in one instance a thinner film (≈350 nm) was employed. Thickness of samples were measured using a Dektak 3 surface profilometer as a function of withdrawing speeds in order to establish calibration curves. The thicknesses measured were in good agreement with values extracted from the transmittance spectra using transfer-matrix method.

Time-resolved spectroscopy and mapping: An optical microscope (Zeiss AX10 Imager.Z1m) was used to produce polychromatic light with a tungsten bulb, focusing light on the sample and collecting the transmitted or reflected beam with an objective. A light pipe collected the light which was analyzed with a spectrometer (ORIEL instrument 77400) and a CCD camera (Andor Technology DV420A-OE). To improve the signal-to-noise ratio, double optical cavities were used based on silicon/silicon oxide substrates as shown in the inset. Spectra were captured every 30 ms over a range between 450 to 750 nm. The temperature of the sample was controlled with a hot-plate (Linkam LTS420). When samples were ‘rested’ between heating scans, we did so for 5 min. This was the time necessary to ensure that the sample was fully cooled to room temperature; no change in refractive index was observed in these 5 min, as can be deduced from the fact that the refractive index after the resting times at room temperature is identical to the refractive index measured after the 10-s heating step (Figs. 1C). Note: Longer resting times could have been used as the refractive index and thickness of our hybrid films are, in the solid state, stable over months, if not years. Built-in apertures were adjusted to control the spot size. A schematic of the setup is shown in **Fig. S2**. For steady-state mapping of samples deposited on glass, integration times were increased to further improve signal to noise.

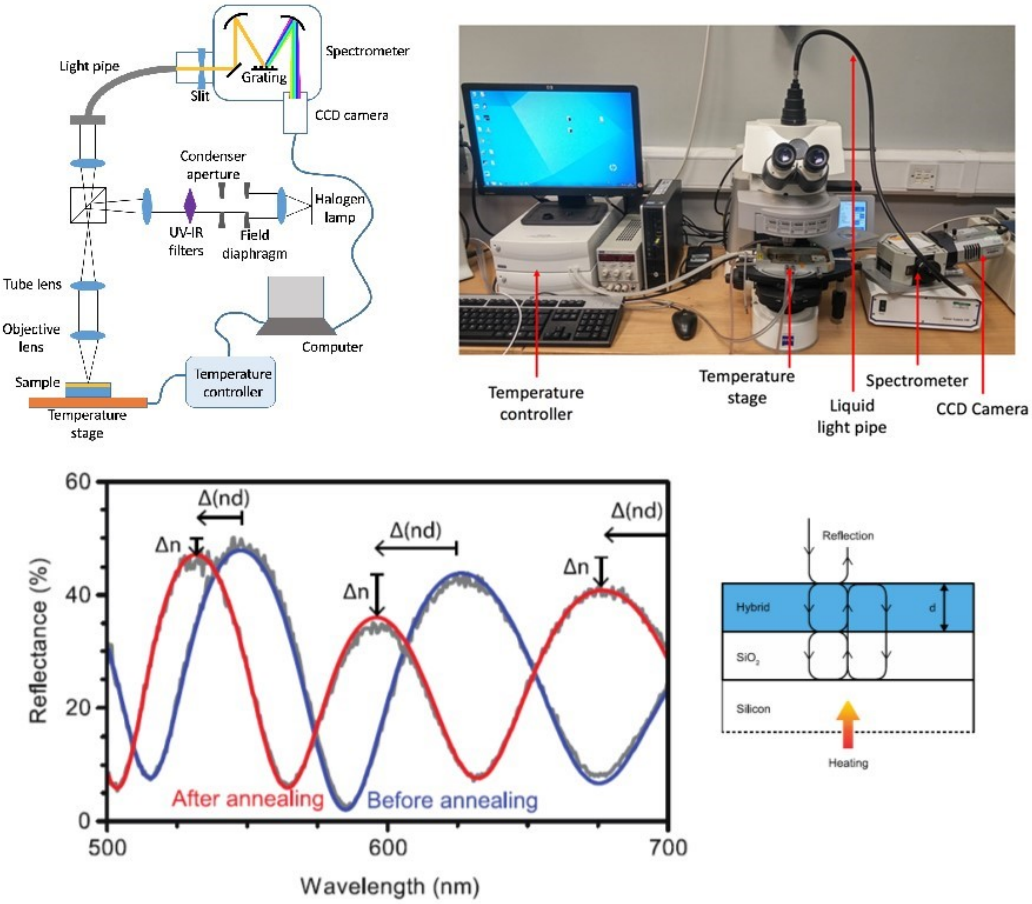

Fig. S2. Top: *In-situ* setup for measuring transmittance or reflectance of thin films as a function of temperature. A spectrometer and CCD camera are linked to a microscope while a Linkam hotplate is used underneath the optical objective. The camera is able to capture a spectrum every 30 ms upon heating with good signal-to-noise ratio. **Bottom:** Reflectance spectra demonstrating the film response to annealing. The change in free-spectral range is associated with changes in optical path length, $n{\cdot}d$. The change in refractive index, Δn is responsible for changes in amplitude. Film properties are extracted using non-linear least square fits. [Note: a double cavity, see inset, was used to conduct the *in-situ* measurements during hybrid film annealing to increase signal-to-noise ratio].

Optical modelling: Coherent transmittance and reflectance were calculated using a Transfer Matrix Method (TMM).[41] The complex refractive index and thickness of the hybrid layers were used as inputs. Since the substrates used were of thicknesses (≈1 to 2 mm) much greater than the wavelength of light contributions from the substrate-air interface were included in an incoherent manner.[41] When fitting the experimental data, the TMM model was used as an objective function with refractive index and thickness as fitting parameters. The MATLAB Levenberg-Marquardt algorithm[42,43] was implemented to minimize the TMM model chi-squared value until a local minimum was found. Fitting results were cross-checked with thicknesses from profilometry, expected refractive indices as well as visual inspection of functional overlap. To reduce the number of free parameters at one time, substrate indices were fit first in the absence of any sample film.

COMSOL Multiphysics was used for finite-element method calculations of normalized electric fields of fundamental modes. The modes chosen were TE-like modes with electric field vectors primarily parallel to the plane of the film. Calculations were made at a wavelength of 550 nm, and the following refractive indices are quoted at that wavelength. The top layer was air at $n=1$, a 1 micron wide core was used with refractive indices 1.73 and 1.68 for large $\Delta n = 0.1$ and small $\Delta n = 0.05$ cases respectively. A core height of 575 nm and side cladding height of 660 nm were used to match thicknesses achieved after and before annealing. Finally, a substrate of glass was included with refractive index 1.52. Perfectly matched layers were added on the sides of the geometry to absorb reflections within the calculation to simulate a significantly wide film (much greater than the wavelength of 550 nm).

Photonic curing: The photonic curing was carried out using a Speedotron xenon flash lamp system (105 CC light unit, 4803CX LV power supply). The energy of each xenon flash was set to 4.8 kJ. The flashes were 1- 1.6 ms in length, at a rate of 0.125 Hz onto the sample stage 1 cm away from the bulb. Note that the choice of metal plays an important role in photonic curing.[3] Chromium and titanium are, in principle, more suitable materials due to their higher absorbance compared to aluminium used here. Thus, further improvements in speed and resolution may be achieved with such metal patterns.

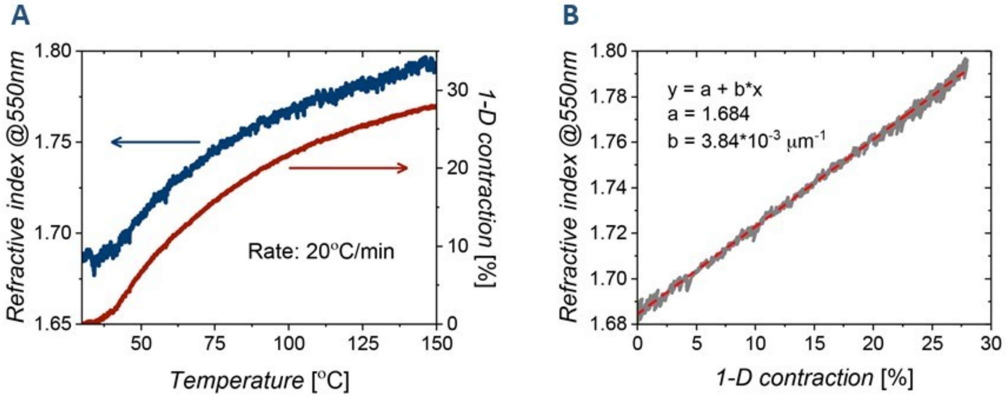

Fig. S3. *In-situ* characterization of hybrid film (≈630 nm-thickness) during annealing using a heating rate of 20 ˚C·min^{-1}. The samples were deposited on silicon oxide/silicon substrates; the optical response was measured every 30 ms and analyzed with TMM. **A.** Temperature-resolved refractive-index- and 1-D-contraction- plots that can be used to extract the required annealing temperature to achieve a specific refractive index (a specific shrinkage). **B.** Refractive-index, *n*, versus 1-D-contraction. The curve can be fitted using a linear equation (see red dotted line; parameter from fitting are shown in inset), allowing to extract the refractive index from thickness measurement and vice versa.

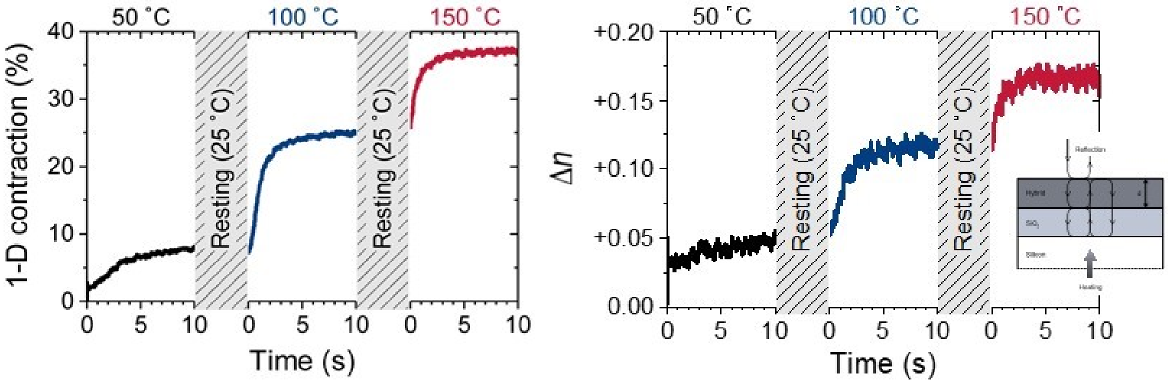

Fig. S4. Evolution of thickness, *d* (left), and refractive index, *n* (right), during three consecutive *in-situ* measurements of the same hybrid film (thickness ≈350 nm), annealed in sequence at 50, 100 and 150 ˚C. The annealing time at each temperature was 10s. After each cycle, the sample was removed from the hot stage and cooled to room temperature. During heating, the hybrid's refractive index increases and saturates after ≤5 seconds, depending on the heating temperature. Note: The hybrid was deposited on silicon oxide/silicon substrates to create a double optical cavity, see inset in right panel, to reduce errors in the fitting of the optical response during annealing and improve thermal conductivity through substrate. Reflectance spectra were recorded every 30 ms. *n* and *d* were extracted using TMM fully-automated fitting loop. The refractive index changes are additive: i.e., annealing a sample to 100 °C after a first heat treatment at 50 °C adds to the Δ*n* achieved in the first step. This leads to a Δ*n* of close to +0.15. The thinner film thickness of ≈ 350 nm used in this experiment, compared to ≈630 to ≈670 nm used in the other measurements, may contribute to this effect.

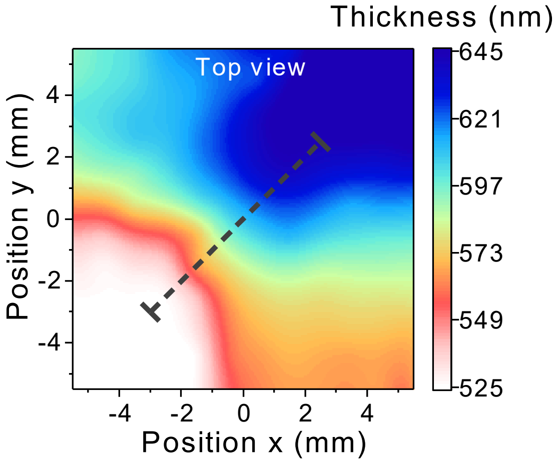

Fig. S5. Thickness mapping (top view) of a 60 vol% titanium oxide hydrate/PVAl hybrid sample (initial thickness: ≈645 nm) after three successive annealing cycles where a pre-heated metal stamp was brought into contact with the sample for 5 seconds, as outlined in the main text, resulting in 1-D contraction and refractive index increase in the exposed areas. In this specific example, four different areas were produced with different *n* (see Fig. 2B) and *d*. The green dotted line corresponds to a refractive-index gradient that is produced across the diagonal of this array, as already mentioned in the main text as well. Spectra were measured and analyzed with TMM to deduce *n* and *d*.

References:

1. M. Russo, M. Campoy-Quiles, P. Lacharmoise, T. A. M. Ferenczi, M. Garriga, W. R. Caseri, N. Stingelin, *J. Polym. Sci. Part B Polym. Phys.* **2012**, *50*, 65.
2. S. Bachevillier, H.-K. Yuan, A. Strang, A. Levitsky, G. L. Frey, A. Hafner, D. D. C. Bradley, P. N. Stavrinou, N. Stingelin, *Adv. Funct. Mater.* **2019**, *29*, 1808152.
3. N. Twyman, K. Tetzner, T. Anthopoulos, D. Payne, A. Regoutz, *Appl. Surf. Sci.* **2019**, *479*, 974.